CONSTRUCTION OF THE VELOCITY MAPS OF THE PN AND SN WAVES FOR ROMANIAN TERRITORY, USING THE TWO STATIONS METHOD. POSSIBILITIES TO USE THIS DATA IN MODELING THE STRUCTURE AND LITHOLOGY OF THE LITHOSPHERIC MANTLE ON THE TERRITORY OF ROMANIA

NICULICI Eugen Laurențiu, DINU Luminița

Abstract. The study of the propagation velocity of the refracted waves on the upper surface of the lithospheric mantle is one of the best methods used to model the lithological composition and mantle structure. The velocity determination method was proposed by PRESS & EWING (1954) and we have added a method to correct the effects of the earth crust. Based on this study capitalizing data from the stations on the territory of Romania and on the territory of the neighbouring states, we were able to identify a significant variation of the propagation velocity of the seismic waves in the lithospheric mantle, which suggests an important variation of its lithology. Emplacement of the volcanic area in Persani on a zone of minimal seismic wave velocities in the mantle implies the possibility of having in this area magmatic basins that can be reactivated in the future. The maximum velocity portion of the seismic waves at the centre of the Vrancea seismogenic area suggests the existence in this place of mantle formations with totally different physical properties and lithology compared to the adjacent areas.

Keywords: Pn, Sn velocity, structure, lithology, upper mantle.

Rezumat. Construcția hărților vitezelor undelor Pn şi Sn pe teritoriul românesc, folosind metoda celor două staţii. Posibilităţi de utilizare a acestor date în modelarea structurii şi litologiei mantalei litosferice pe teritoriul României. Studiul vitezei de propagare a undelor refractate pe suprafaţa superioară a mantalei litosferice este una dintre cele mai bune metode utilizate pentru modelarea compoziţiei litologice şi a structurii mantalei. Metoda de determinare a vitezei a fost propusă de PRESS & EWING (1954) şi am adăugat o metodă de corectare a efectelor scoarţei terestre. Pe baza acestui studiu realizat pe datele de la staţiile de pe teritoriul României şi pe teritoriul statelor învecinate, am putut identifica o variaţie semnificativă a vitezei de propagare a undelor seismice în mantaua litosferică, ceea ce sugerează o variaţie importantă. a litologiei sale. Amplasarea zonei vulcanice de la Perşani pe o zonă de viteze minime a undelor seismice în manta presupune posibilitatea de a avea în această zonă bazine magmatice ce pot fi reactivate în viitor. Porţiunea de viteză maximă a undelor seismice în centrul zonei seismogene Vrancea sugerează existenţa în acest loc a formaţiunilor de manta cu proprietăţi fizice şi o litologie total diferită faţă de zonele adiacente.

Cuvinte cheie: Viteza Pn, Sn, structura, litologie, manta superioară.

INTRODUCTION

The Pn and Sn waves are refracted waves propagating along the Mohorovicic surface through the lithospheric mantle. They can be used to determine the propagation velocities of the elastic waves in the upper part of the lithospheric mantle. Considering the existence of a tight correlation between the lithological composition of the mantle and the propagation velocity of the elastic waves, we can use this information in the processes of modeling the composition and structure of the mantle, especially if we have data on propagation velocity anisotropy (Fig. 1).
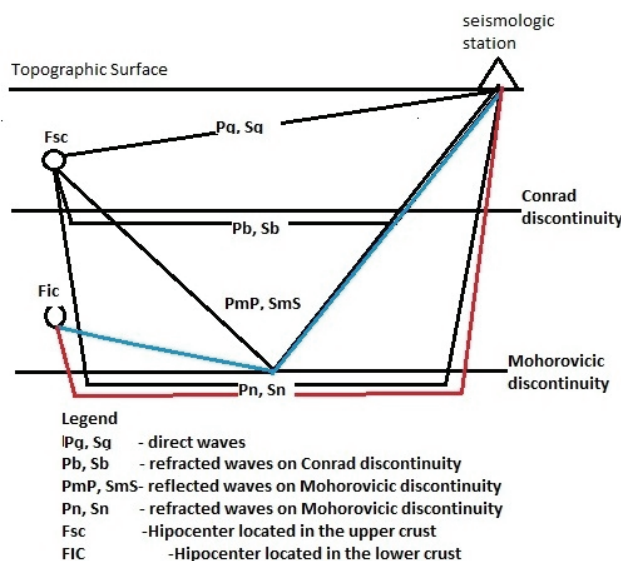

Figure 1. Outline of the reflected and refracted waves on the main discontinuities in the Earth's lithosphere.

The present paper aims to present the distribution of wave propagation velocities at the Mohorovicic discontinuity level, without presenting anisotropy data, as the wave propagation velocities for the same site could not be calculated, using earthquakes located in directions perpendicular to each other.

The results thus obtained will be presented in the form of velocity maps of the seismic waves and interpreted in terms of lithology of the structural units that make up the mantle on the territory of Romania. The main purpose of such a study is to improve the knowledge of the compositional and structural characteristics of the mantle, in the context in which this is not achievable by direct investigation.

THE CURRENT STATE OF RESEARCH IN THE STUDIED AREA

Internationally, the technique used for this work was used in 2004 to build the regional-scale maps for the contact area between the Arabian Plate, the African Plate and the Eurasian Plate (AL LAZKI et al., 2004). Internally in 2004 maps of Pn and Sn speeds were made for the Vrancea area and the adjacent areas, these being presented on the website of the Faculty of Geology and Geophysics of the University of Bucharest by Professor Marian Ivan, but without continuing the research in this direction (IVAN, 2004).

The degree of detail in the work by AL LAZKI et al. (2004) is much lower, so that the present paper brings new information regarding the distribution of seismic velocities for the lithospheric mantle on the Romanian territory.

There are important variations of the Pn wave velocities including in the eastern part of the Romanian territory, where AL LAZKI et al. (2004) identified an area of high velocities (over 8 km/s). Another novelty is the use of Sn shear waves, which together with the Pn waves can provide more information regarding the structure and lithology of the mantle.

METHOD DESCRIPTION

The determination of the Pn and Sn waves velocities by the two stations (PRESS & EWING, 1954) is done by calculating the propagation velocity of the refracted waves on the Mohorovičić discontinuity on the distance between two receivers located in the same direction in relation to the epicenter. The calculated speed value is reported to the half of the distance between the two stations. Epicenter distances and azimuths between seismological stations and event epicenter are calculated using the DistAz program, downloaded from the airy.ual.es/www/DistAz_english.htm site. Arrival times were determined using the WinQuaqe program. The maximum epicentral distance for which the Pn velocities can be calculated is 850 Km.

The WinQuaqe application calculates the acoustic wave travel times between the epicenter and the receiving station, based on the IASP91 Model. The arrival times of the Pn and Sn waves are determined by finding the arrival times of those waves on all the components recorded in each station. In some cases, this is not possible due to the noise recorded on some components (usually the horizontal ones). It is believed that the stations are located in the same direction with respect to the epicenter when the difference between their azimuths is less than 5 degrees. The velocity is calculated by dividing the distance between the two stations by the time difference between the arrivals of the same wave at the two stations, after correction of crustal effects. This calculation method is used to compute propagation velocities in the case of stations located more than 100 km away from the epicenter, in which case it is considered that the difference between the arrival times of the two stations is due exclusively to the propagation of the waves through upper lithospheric mantle. The resolution with which the velocity is determined depends on the density of the seismological network stations and their distribution. The weight given to a calculated velocity is inversely proportional to the distance between the stations for which the velocity is calculated and proportional to the signal / noise ratio observed at the pairs of stations used. Also, pairs of stations that are located at distances less than 10 km from each other are not taken into account, since the possible errors in determining the arrival times of the Pn and Sn waves are comparable to the travel times of these waves on this distance. If we can determine the velocities of elastic waves emitted by earthquakes whose epicenters are located in directions approximately perpendicular to the receiving seismic station, the wave propagation anisotropy can also be determined.

USED DATA

In order to obtain an accurate picture of the upper part of the lithospheric mantle, we use the refracted waves that propagate along the Mohorovičić discontinuity, within the mantle. For this purpose, we use data of Pn and Sn waves arrival times coming from the seismic stations in the networks of Romania, Serbia, Bulgaria, Hungary and the Republic of Moldova, for the stations that fall into the distance domain that allows the detection of these waves. Due to the fact that some stations in the neighboring countries and in Romania were either very noisy, not allowing the identification of arrival of the Pn and Sn waves, or they are located at distances greater than 850 km from the epicenters of the events used, in the end we could only use 60 of the 117 stations belonging to the networks of the 5 countries. Finally the following stations were used: BSZH, BUD, CSKK, MORH, PSZ, SORM, BEO, BLKB, DJES, FRGS, ARR, BAIL, BANR, BISRR, BMR, BUR05, BUR32, BURAR, BZS, CJR, COPA, CVD1 , DEV, DJES, DRGR, ELND, GHRR, GZR, HERR, HUMR, IAS, ICOR, KALB, LEHL, LOT, LOZB, MDVR, MILM, MLR, PLOR, PLOR1, PLOR2, PLOR3, PLOR4, PLOR5, PLOR6, PLOR7 , PLVB, PSZ, PUNG, RASA, RAZG, SIRR, SLCR,

SULR, TESR, TRISU, VLAD, SEE, VRI,. The earthquakes used had hypocenters at depths between 5 and 30 km and magnitudes of over 5 degrees on the Richter scale. The data were downloaded in miniseed format from the website http://145.23.252.222/eida/webdc3/ and contain information for a the period that starts with 2 minutes before the event takes place and ends at 10 minutes after the moment of its occurrence. The velocities were calculated for a number of 169 pairs of stations, covering about 75% of the national territory, except for the north of Maramureș, Bucovina and Dobrogea.

OBTAINED RESULTS

From all the pairs of stations for which we calculated the velocities were retained only those for which the velocity values fall within the range at the mantle level presented in the IASPEI91 model. Also, the pairs of stations with the distance between stations less than 10 km were eliminated (the pairs formed by stations located in the Array devices from Ploștina and from Bukovina). We also eliminated from the calculation, also due to the small distance, the pairs of stations formed by the Vrâncioaia station (VRI) with the stations in the Ploștina area (PLOR, PLOR1, PLOR2, PLOR3, PLOR4, PLOR5, PLOR6). We built the velocity maps of the Pn (Fig. 2) and Sn (Fig. 3) waves using the data in Table 1, interpolated using the minimum curvature method in a network with 12444 knots and with an equidistance of 4998 m per E-V direction and 4959 m on the NS direction. The calculated maximum Pn velocity is 8.8 km/s and can be found in several areas of the Moldavian Platform (part of the East-European Platform), the south and center of the Romanian area of the Moesian Platform. The minimum Pn velocity calculated is 6.5 Km/s and is found in the curvature of the Eastern Carpathians, in the Panonic Depression, and in the Vedea-Pietroșani area in the south of the Romanian area of the Moesian platform (Fig. 2). The maximum velocity Sn calculated is 5.3 km/s, in the south of the Southern Carpathians, in the area of the forearm near their curvature and in the south of the Pannonian depression (Fig. 3). The minimum calculated Sn velocity is 3.5 km/s, at the boundary between the External Foredeep and the Scythian Platform, in the northern area of the Pannonian depression, in the north of the Eastern Carpathians, in the south of the Transylvanian Depression, near Sâmbata de Sus and in the Moesian Platform, at about 30 km west of Bucharest.

In general it can be observed that the areas with the highest velocities of the Pn and Sn waves correspond to the platform areas. The areas with the lowest velocities generally overlap with the orogen areas and those located along the active tectonic elements. An exception in this respect is the Vrancea seismogenic area, where, in the center, the Pn velocities are among the highest (over 8.13 km/s) while the Sn velocities are relatively low (4.2–4.5 km/s). At the southern and northern limits of this zone there are low velocity zones on both the Pn and Sn maps. The northern limit of these low-velocity zones is near the Trotus Fault and the southern one near Ramnicu Sarat.
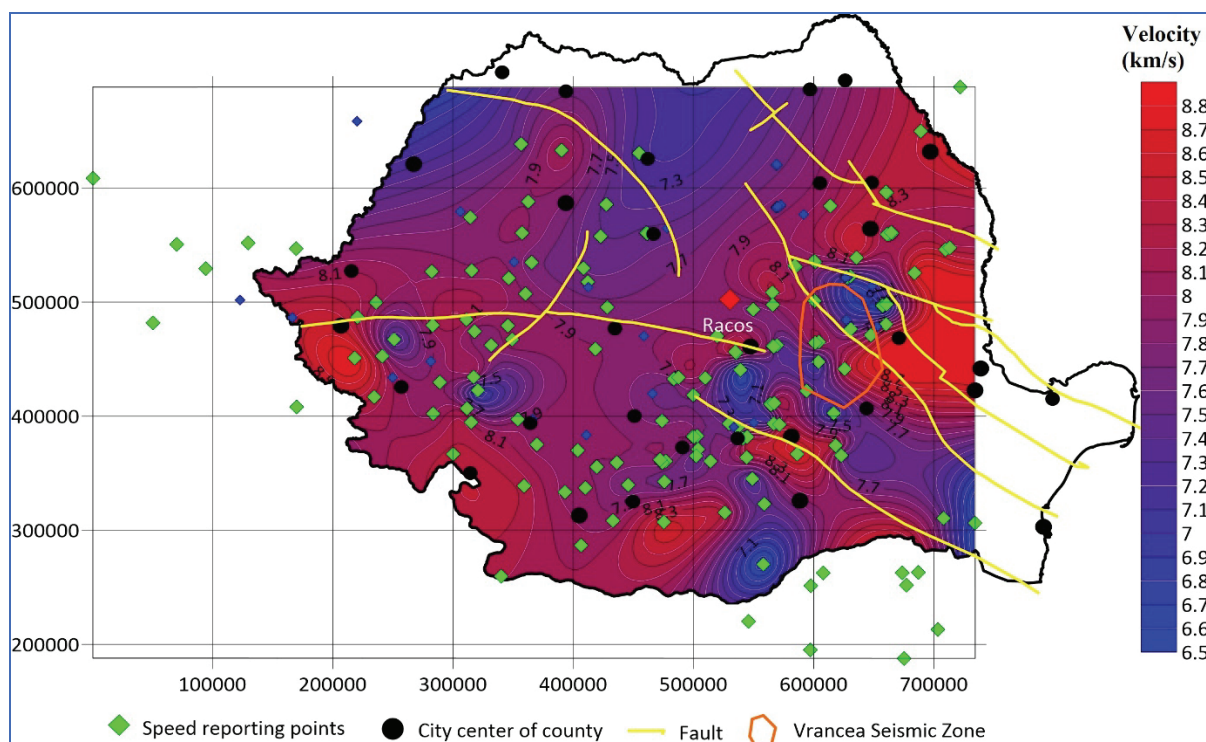

Figure 2. Map of the distribution of Pn wave velocities on the Romanian territory.
The map shows the main structural elements that affect the Earth's crust on the Romanian territory.
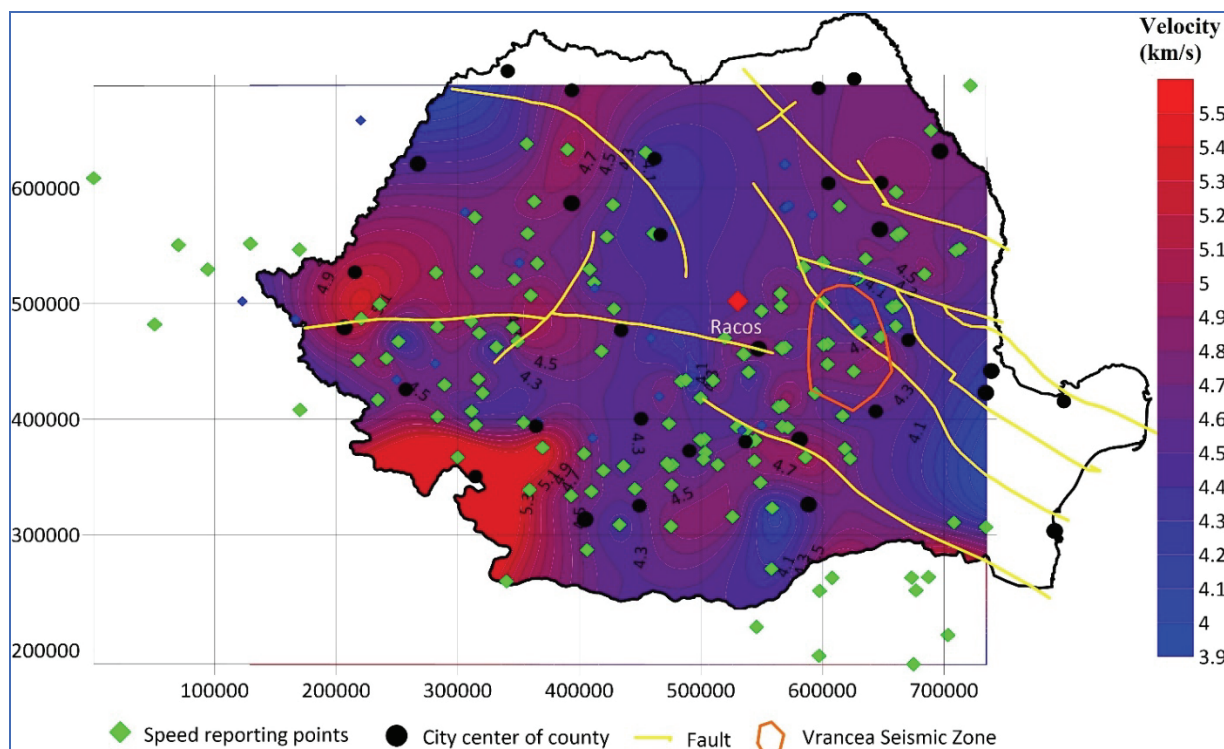
Figure 3. Map of the distribution of Sn wave velocities on the Romanian territory.
The map shows the main structural elements that affect the Earth's crust on the Romanian territory.

DISCUSSIONS AND CONCLUSIONS

By observing the Pn (Fig. 2) and Sn (Fig. 3) maps, there is an obvious inhomogeneity of the lithospheric mantle for the entire surface for which the velocities could be calculated. We find a good overlap of the accentuated velocity gradient areas with the areas crossed by crustal tectonic elements, which in this case also seem to affect the lithospheric mantle.

An interesting fact is that, for the Vrancea area, we can find an overlap of the maximum anomaly of the Pn wave velocity (Fig. 2), oriented in the NW-SE direction with an anomaly with much lower Sn velocities (Fig. 3), oriented E-V. This anomaly characterizes the center of the seismogenic zone. This overlap can be considered to be produced by a compositional variation, in the sense of the presence in this area of the garnet pyroxenitic formations (similar to the eclogites), probably due to the high pressure metamorphism of crustal formations at great depths, in a continental collision zone (NICULICI, 2012a).

Another interesting element is the presence of a minimum anomaly of the Pn and Sn velocities in the Quaternary volcanite area of the southern Perșani mountains, which suggests the existence of melts in the mantle in this area, which would represent a magmatic basin that could be reactivated in the future. This fact is also supported by the results of the previous laboratory studies carried out on samples from the ultra-basic xenoliths from Racoș and from the quarries on the Bogatii valley (NICULICI, 2012). The corrections applied to these data were made with the help of the Macro presented in the paper of HACKER & ABERS (2004). Thus, the velocity determinations with the help of the ultrasounds performed in 2011 in the process of conducting the doctoral thesis (NICULICI, 2012a), did not show decreases in velocity below the normal limits for the lithospheric mantle. On this basis, the decrease of seismic velocities in this area can be due the presence of some magmatic basins and not on account of the water content present in the olivine from these formations, highlighted by FALUS et al. (2008) and KOVÁCS et al. (2018).

The study of the propagation velocity of the seismic waves refracted at the interface of the crustal mantle (Mohorovičić discontinuity) together with the study of the propagation velocity of the acoustic waves through ultrabasic rocks, similar to those that compose the lithospheric mantle, can provide important information for the construction of physical and lithological models with a high confidence for the lithospheric mantle. The use in such a study of the anisotropy data of the mantle obtained by SKS splitting methods (IVAN et al, 2008) may lead to an improvement of the model, as it could bring information about possible lithological variations, given that the regional tectonic structure remains the same. In general, seismological data are the basic element of qualitative and quantitative investigation for the deep structure of the Earth. To obtain an improved model of the lithospheric mantle structure and lithology, seismological data can be associated with gravimetric data (Bouguer anomaly) (BESUTIU, 2006) and with data on the density of rocks that make up the mantle of the earth, determined on ultra-basic xenoliths.

Generally it can be observed that the areas with the highest velocities of the Pn and Sn waves correspond to the platform areas. The areas with the lowest velocities generally overlap with the orogenic areas. The areas along the active tectonic elements are characterized by an accentuated velocity gradient, either lower, as in the case of the Trotuș Fault or

higher, as in the case of the Intra-Moesian Fault. An exception in this respect is the Vrancea seismogenic zone, where the Pn velocity is the highest (over 8.13 km/s), while the Sn velocity is relatively low (4.2–4.5 km/s). An area with minimal velocity is that of the Quaternary volcanoes in the southern Perşani Mountains. In this case, both Pn and Sn velocities are small, with values around 7.3 km/s, respectively 4.2 km/s. In this case, the velocities are very close to those characteristics of the basaltic crust layer, which suggests either a major change in the composition in this area, or an increase in entropy in this area, due to the probable existence of the larger geothermal gradients, associated, as mentioned, to magmatism.

REFERENCES

AL-LAZKI A. I., SANDVOL E., SEBER D., BARANGI M., TURKELLI N., MOHAMAD R. 2004. Pn tomographic imaging of mantle lid velocity and anisotropy at the junction of the Arabian, Eurasian, and African plates. *Geophysical Journal International*. Oxford University Press. Oxford U. K. **158**: 1024-1040.

BESUTIU L. 2006. Alternative geodynamic model for the Vrancea intermediate-depth seismicity: the unstable triple junction : in Rus, T. (Ed.): *Geodynamic Studies in Romania. Vrancea Zone. A Monograph, Reports on Geodesy*. Warsaw University of Technology. **6**(81): 73-95.

PRESS F. & EWING M. 1954. Waves with Pn and Sn velocitz at great distances. *Proceedings of the National Academy of Sciences of the United States of America*. Washington D. C. **41**(1): 24-27.

FALUS G., TOMMASI A., INGRIN J., SZABO C. 2008. Deformation and seismic anisotropy of the lithospheric mantle in the southeastern Carpathians inferred from the study of mantle xenoliths. *Earth and Planetary Science Letters*. Elsevier. Amsterdam. **272**: 50-64.

HACKER B. R. & ABERS G. A. 2004. Subduction Factory 3: An Excel worksheet and macro for calculating the densities, seismic wave speeds, and H2O contents of minerals and rocks at pressure and temperature. *Geochemistry, Geophysics, Geosystems*. Wiley. Hoboken. **5**(1), Q01005, doi:10.1029/2003GC000614.

IVAN M. 2004. *Pn and Sn velocity maps for Vrancea area and adjacent areas*. www.gg.unibuc.ro, unpublish work (accessed: January 14, 2023).

IVAN M., POPA M., GHICA D. 2008. SKS splitting observed at Romanian broad-band seismic network. *Tectonophysics*. Elsevier. Amsterdam. **462**: 89-98.

KOVÁCS I., PATKÓ L., FALUS G., ELŐD ARADI L., SZANYI G., GRÁCZER Z., SZABÓ C. 2018. Upper mantle xenoliths as sources of geophysical information: the Perşani Mts. area as a case study. *Acta Geodaetica et Geophysica*. Springer. Heidelberg. **53**: 415-438.

NICULICI E. L. 2012. Elastic waves velocities and the anisotropy of the xenoliths from Racos alkaline basalts. *Revue Roumaine de Geophysique*. Editura Academiei. Bucuresti. **56-57**: 65-71.

NICULICI E. L. 2012a. *Geological model of the Mohorovicic Discontinuity for the territory of Romania based on the maps of Pn and Sn speeds*. Ph. D. thesis. University of Bucharest. DOI: 10.13140/RG.2.2.13337.11368.

Niculici Eugen Laurenţiu
Geological Institute of Romania 1st Caransebeş Street, 012271 - Bucharest, Romania.
E-mail: niculicie@yahoo.com

Dinu Luminiţa
Geological Institute of Romania 1st Caransebeş Street, 012271 - Bucharest, Romania.
E-mail: luminita_iancu84@yahoo.com

Appendix

Table 1. Average rates of waves Pn and Sn results for pairs of stations used for earthquakes from Albania and the NW Balkan region.

No.	Pairs of stations	$N_{Stereo70}$ (m)	$E_{Stereo70}$ (m)	VPn (km/s)	VSn (km/s)
1	KALB-ELND	187872.8	675003.9	7.983016	4.675088
2	RAZG-ELND	195171.1	597197.1	8.873045	5.296057
3	KALB-LOZB	213140.1	703124.4	7.297032	4.174631
4	RAZG-PLVB	220178.9	545842.7	7.692644	4.359468
5	PLVB-ICOR	251305.6	597581.3	8.120782	4.475635
6	LOZB-ICOR	251858	676940.7	8.248682	4.318899
7	BLKB-BAIL	259767.1	340019.6	8.206443	5.316761
8	PLVB-CVD1	262581.4	607868.3	8.222604	5.052137
9	RAZG-ICOR	262882	673423.9	8.724326	4.628957
10	LOZB-CVD1	263259.5	687093.2	8.435109	5.579855
11	PLVB-LEHL	270282.5	557942.5	6.520404	4.029421
12	BLKB-HUMR	286816	406397.6	8.047225	4.468152
13	CVD1-ICOR	306491.1	734229	6.837414	4.199682
14	HUMR-VLAD	307298	475369.7	8.526194	4.634614
15	HUMR-BAIL	308710.4	433063	7.969288	4.13544
16	CVD1-RASA	310601.1	708105.2	7.486695	4.171472
17	SULR-VLAD	315636	526039	8.302055	4.556347
18	COPA-SULR	323072.6	558667.8	7.464117	3.77895
19	BLKB-ARR	333699	393156.5	7.965734	4.58052
20	BLKB-VOIR	337331	409911.6	7.971453	4.47031
21	LOT-BLKB	338804.5	359059.5	8.262619	5.206876
22	BLKB-MLR	339705	445701	7.7051	4.404233
23	BLKB-BISRR	342852.8	475903.5	7.619024	4.426626
24	SULR-HUMR	345215.1	548940.2	7.303717	4.520496
25	BAIL-ARR	355536.7	419680.1	7.875656	4.345858
26	BAIL-VOIR	359237.4	436361.9	7.895682	4.244745
27	BLKB-PLOR5	359527.5	473986.7	7.907092	4.38587
28	BLKB-PLOR4	359529.2	473590.7	7.943327	4.407203
29	BLKB-PLOR	359529.2	473590.7	7.922806	4.403795
30	BLKB-PLOR1	359529.2	473590.7	7.938582	4.494145
31	BLKB-PLOR2	359530.8	473194.7	7.916469	4.396871
32	BLKB-PLOR7	360086.4	473197.1	7.951249	4.556293
33	MLR-VLAD	360599.9	513980	7.721365	4.526495
34	BLKB-VRI	360627.9	476762.8	7.775114	4.410564
35	MLR-BAIL	361758.2	472016.6	7.583392	4.214215
36	BISRR-VLAD	364069.5	544047.5	8.234221	4.626294
37	BISRR-BAIL	365029.7	502100.8	7.500977	4.269472
38	SLCR-TRISU	365654.5	622781.6	7.605697	4.42057
39	SLCR-VLAD	366718.8	585962.8	8.609054	4.8633
40	DJES-HERR	367067	299904.4	8.33702	6.525783
41	PUNG-ARR	370206	403652.7	7.971165	4.599775
42	BLKB-GHRR	371141.6	503680	7.677327	4.361388
43	COPA-SLCR	374460.4	618264.3	8.298076	4.539879
44	LOT-PUNG	375256.8	369744.3	7.955229	5.505619
45	PLOR2-VLAD	380717.8	541169.8	7.801749	4.514532
46	BAIL-PLOR5	381696.3	500122.7	7.847336	4.231219
47	PLOR4-BAIL	381696.4	499728	7.890516	4.255239
48	PLOR-BAIL	381696.4	499728	7.866052	4.251399
49	BAIL-PLOR1	381696.4	499728	7.884857	4.353532
50	PLOR2-BAIL	381696.4	499333.4	7.858308	4.243101
51	VLAD-VRI	381852.8	544714.1	8.23792	4.720463
52	BAIL-PLOR7	382252	499333.5	7.899965	4.424192
53	BAIL-VRI	382808.1	502884.5	7.692113	4.26145
54	HUMR-MLR	390135.7	536773.7	7.325794	4.466886
55	GHRR-VLAD	392653.4	571428.6	8.17336	4.479987
56	GHRR-BAIL	393432	529664.4	7.590876	4.227215
57	HUMR-BISRR	393713	566689.5	7.174815	4.379271
58	GZR-DJES	394962.5	314975.5	8.103464	4.434573
59	BLKB-TESR	396196.2	473743.7	7.769367	4.385773
60	LOT-DJES	397274	354047.6	7.912606	4.440523
61	GZR-MDVR	402086.4	283282.9	7.995722	4.714459
62	SULR-BISRR	402769.7	616557.2	7.03914	4.234786
63	GZR-HERR	406743.2	311385.7	8.040997	4.146727
64	BANR-BEO	408106.1	170046.1	7.68643	3.976731
65	PLOR2-HUMR	410351.2	563764.2	7.781265	4.32312
66	PLOR4-HUMR	410355.2	564157.1	7.835765	4.344199

No.	Pairs of stations	$N_{Stereo70}$ (m)	$E_{Stereo70}$ (m)	VPn (km/s)	VSn (km/s)
67	PLOR-HUMR	410355.2	564157.1	7.794674	4.337373
68	HUMR-PLOR1	410355.2	564157.1	7.826244	4.522115
69	HUMR-PLOR	410355.2	564157.1	7.708699	4.340622
70	HUMR-PLOR5	410359.2	564549.9	7.763357	4.301646
71	HUMR-PLOR7	410906.7	563758.6	7.851685	4.653901
72	HUMR-VRI	411499	567287.9	8.137303	4.752659
73	BZS-MDVR	416756	234250.2	8.273893	4.389749
74	TESR-BAIL	418363.7	499730.5	7.694636	4.250065
75	GHRR-HUMR	422395.4	593838.7	7.626274	4.399369
76	DJES-DEV	422598.4	320495.2	6.889612	4.296655
77	DEV-MDVR	429696.3	288938.4	7.928131	4.449863
78	PUNG-TESR	432830.3	483682.9	7.738321	4.36147
79	BLKB-IASR	433371.8	509907.8	7.94375	4.443507
80	VOIR-ARR	433932.3	487599.4	8.020401	3.716016
81	HERR-DEV	434376.1	316914.7	7.959598	4.532722
82	MLR-VOIR	440708.6	539217.3	6.631893	4.107061
83	MILM-VLAD	441289.1	625622.9	8.228472	4.584936
84	MLR-BISRR	447561.3	604010.1	7.104838	4.5774
85	BZS-BANR	450844	218086.9	8.780832	4.627154
86	MDVR-SIRR	452622.4	241242.1	8.193826	4.7227
87	BAIL-IAS	456239.4	534830.5	8.274642	4.549798
88	BUR5-BLKB	458903.7	418259.5	7.904514	4.446063
89	PLOR2-VOIR	460935.6	565980.7	7.796799	4.240364
90	PLOR4-VOIR	460939.8	566370.3	7.881996	4.272686
91	PLOR-VOIR	460939.8	566370.3	7.817593	4.262437
92	VOIR-PLOR1	460939.8	566370.3	7.86704	4.545976
93	VOIR-PLOR5	460943.9	566760	7.768764	4.209066
94	VOIR-PLOR7	461491.2	565974.8	7.90705	4.756325
95	VOIR-VRI	462084.8	569475.4	7.390813	4.288135
96	GZR-DEV	462309.2	331771.3	7.801838	4.018037
97	MLR-PLOR2	464182.9	601006.4	8.058724	4.478278
98	MLR-VRI	465351.9	604493.2	8.107757	4.439377
99	BSZH-BAIL	467235.3	251210.6	7.333903	3.96582
100	DJES-CJR	467424.1	349051.4	7.97596	4.722854
101	PUNG-IASR	470063.1	519578.3	7.942722	4.431856
102	HUMR-MILM	471226.8	647598.7	8.175578	4.575848
103	CJR-MDVR	474380.7	317697.1	7.852821	4.479752
104	GHRR-MLR	476407.5	630751.2	7.606281	4.254146
105	CJR-HERR	479185.6	345449.2	7.944162	4.605264
106	DRGR-MDVR	479938	283241.2	8.084808	4.721813
107	GHRR-BISRR	480432.8	660208.7	7.981841	4.062867
108	DRGR-HERR	484588.8	311002.1	8.153337	4.676258
109	BANR-SIRR	486902.9	220496.2	8.27444	5.24089
110	ARR-TESR	493567.1	549740.9	7.760087	4.317975
111	BUR5-PUNG	495451.6	428430.3	7.7427	4.402306
112	GHRR-PLOR2	497028.6	657065.9	6.415802	4.14372
113	GHRR-PLOR4	497038.4	657453.3	6.279363	4.07945
114	GHRR-PLOR1	497038.4	657453.3	6.299151	3.645466
115	GHRR-PLOR	497038.4	657453.3	7.365143	4.606083
116	GHRR-PLOR3	497038.4	657453.3	7.28351	4.320095
117	GHRR-PLOR5	497048.3	657840.8	6.434326	4.205324
118	GHRR-PLOR7	497584.1	657051.8	6.246658	3.395692
119	TESR-VOIR	497608.4	565979.9	7.825791	4.559992
120	GHRR-VRI	498229.2	660524.2	7.021333	4.027782
121	BZS-SIRR	499582.2	235820	8.093631	5.230181
122	TESR-MLR	500856.6	600798.4	7.959598	4.333725
123	CJR-GZR	507184.6	360082.2	7.90697	4.813147
124	SORM-BAIL	508716.4	565474.6	8.312946	4.532272
125	BURAR-DJES	517891.4	412085.4	7.613115	4.274498
126	BUR31-DJES	517891.4	412085.4	7.626521	4.276374
127	DJES-BMR	520850	346490.5	7.958722	4.537561
128	PLOR-TESR	521358.8	627486.8	6.687988	4.240873
129	TESR-PLOR1	521358.8	627486.8	6.595612	3.650782
130	TESR-PLOR5	521366.8	627872.7	6.782987	4.384962
131	TESR-VRI	522534.7	630550.5	7.714743	4.161701
132	MILM-MLR	525563.8	683744.6	8.65665	4.629955
133	BZS-DRGR	526690.2	282177	7.978358	4.831424
134	BMR-MDVR	527822.8	315412.2	7.910738	4.576306
135	BURAR-HERR	529615.8	408398.9	7.592701	4.356743

No.	Pairs of stations	N$_{Stereo70}$ (m)	E$_{Stereo70}$ (m)	VPn (km/s)	VSn (km/s)
136	BUR31-HERR	529615.8	408398.9	7.60659	4.358773
137	IASR-ARR	531181.6	584888.1	7.926043	4.338454
138	DEV-CJR	534859.1	365335.5	7.747793	4.523107
139	IASR-VOIR	535316.2	601005.6	7.91624	4.416321
140	IASR-MLR	538763.6	635595.6	8.336321	4.504581
141	MILM-PLOR6	545860	709689.7	8.389006	4.349987
142	BSZH-BANR	546761.4	169627.9	7.699045	4.445643
143	MILM-VRI	547646.2	713091.5	8.215259	4.40747
144	PSZ-BEO	551857.1	129423.8	7.862266	4.363207
145	BURAR-GZR	557761.3	422633.5	7.498065	4.235728
146	BUR31-GZR	557761.3	422633.5	7.514373	4.238037
147	IAS-PLOR6	559389.6	660850.5	8.337189	4.343493
148	PLOR4-IASR	559420.1	662001.1	7.944875	4.543024
149	PLOR-IASR	559420.1	662001.1	7.999989	4.552681
150	IASR-PLOR1	559420.1	662001.1	7.957526	4.314239
151	IASR-PLOR5	559430.3	662384.7	8.042907	4.604416
152	IASR-PLOR7	559965.4	661602.8	7.923879	4.169071
153	BUR5-LOT	560169.3	461395.9	7.630983	3.966701
154	BMR-GZR	560608.6	357463.1	7.910969	4.531042
155	IASR-VRI	560613.6	665039.4	8.457364	4.538422
156	BURAR-LOT	560729.9	460632.6	7.475243	4.198014
157	BUR31-LOT	560729.9	460632.6	7.494481	4.200705
158	BZS-BMR	574569.3	314143.1	7.799399	4.588755
159	SORM-ARR	584455.9	613947.9	8.089247	4.439431
160	BURAR-DEV	585488.2	427570.1	7.439634	4.28253
161	BUR31-DEV	585488.2	427570.1	7.458935	4.285367
162	BMR-DEV	588283.5	362696.2	7.897404	4.678628
163	IAS-TESR	596624.9	660246.9	8.334722	4.664701
164	BURAR-CJR	630797.4	454646.5	7.237908	4.128652
165	BUR31-CJR	630797.4	454646.5	7.269031	4.133139
166	BMR-CJR	633302.4	390253.3	8.08007	4.87486
167	BMR-DRGR	638463.5	356644.3	7.57505	4.303358
168	SORM-TESR	649740.4	689086.7	8.408089	4.553946
169	SORM-IAS	688700.7	721674.3	8.472601	4.4623